$Ca_3Al_2Si_2$: An Inorganic Structure Analogous to but Not Isoelectronic with Polyacene†

Jing Li and Roald Hoffmann*

Department of Chemistry and Materials Science Center, Cornell University, Ithaca, New York 14853-1301
(Received: March 17, 1987)

The orthorhombic $Ca_3Al_2Si_2$ structure contains well-separated parallel $Al_2Si_2^{6-}$ chains which extend infinitely in one dimension. The chains resemble structurally the organic polymer polyacene but are more electron-rich. The similarities and the differences in the electronic structure of the two polymers, inorganic and organic, can be appreciated following two constructions of the band structure of the system. Within each chain there are two nonequivalent lattice sites: a twofold one and a threefold one. Three possible ways of assigning Al and Si atoms to these sites are examined. The preferred and realized choice is that all Si atoms reside in the twofold sites, all Al atoms in the threefold ones. A rationale for this is given.

The $Ca_3Al_2Si_2$ structure[1] contains isolated one-dimensional $Al_2Si_2^{6-}$ chains, **1a**. These obviously resemble polyacene, **1b**, an organic polymer. But the electron count is slightly different—Whereas polyacene has 18 valence electrons/unit cell, $Al_2Si_2^{6-}$ has 20. The resemblance and differences of the two polymers is one source of interest in these systems. Another is a choice that is made by the Al and Si atoms in occupying nonequivalent sublattice sites, a general aspect of isomerism in the solid state.

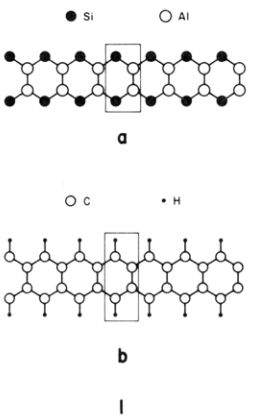

1

Let us discuss the structure first and the rationale behind our electron counting. The $Ca_3Al_2Si_2$ type structure, denoted by $M_3A_2E_2$, crystallizes as an ordered variant of the Ta_3B_4 structure,[2] with two molecular formula units per cell. As shown in **2**, the tantalum atoms in Ta_3B_4 are replaced by the alkaline earth metal, M, and the boron atoms, by equal number of the group IIIA (group 13)[19] element A and the group IVA (group 14) element E. The orthorhombic unit cell of $Ca_3Al_2Si_2$ is drawn in **3**. The short Al–Si, Al–Al contacts, 2.43 and 2.47 Å, are certainly within bonding range. So are the A–A and A–E bond lengths found in all the reported structures of this type. These are listed in Table I. The distances to the alkaline earth atoms in these structures are typically ionic, and so we adopt a Zintl viewpoint, viewing these as $(M^{2+})_3(A_2E_2)^{6-}$. Hence the 20 valence electron count.

The polyacene-like chains of Al and Si in $Ca_3Al_2Si_2$ are apparent in **3**, perhaps even more so in Figure 1, which gives two perspective views of the structure. Ignoring the Ca^{2+}, what we see is a series of double layers of $Al_2Si_2^{6-}$ chains, repeating in the z direction. All the chains are parallel, extended in the x direction. The shortest chain–chain separations are 4.502 and 4.576 Å, as indicated in Figure 1.

Since any two chains are so far apart, we may neglect the chain–chain interactions and simplify our calculations by employing an one-dimensional model. This assumption is not only adopted as a labor-saving device. It actually can be checked by calculating one-, two-, and three-dimensional electronic structures, which for this simple unit cell are fully within the reach of our programs. The band structure along the critical chain directions in the Brillouin zone is shown in Figure 2. The resemblance of the two- and three-dimensional bands to those of the one-dimensional model is remarkable, and it is clearly sufficient to use the simple chain model in the sequel.

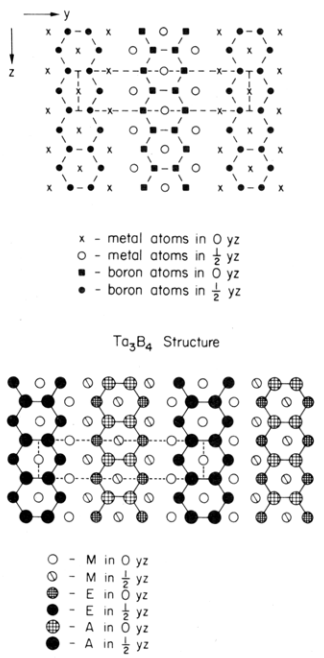

2

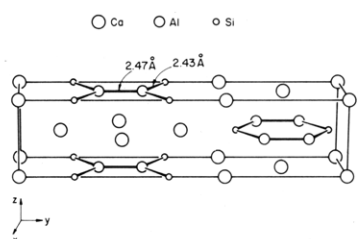

3

We have anticipated here the calculations which form the basis for the body of the paper. We use extended Hückel tight-binding[6]

† This paper is dedicated to Massimo Simonetta, who always looked at structure and, at the same time, thought deeply of bonding.

(1) Widera, A.; Schäfer, H. *Z. Naturforsch. B* **1977**, *32B*, 1349.
(2) (a) Kiessling, R. *Acta Chem. Scand.* **1950**, *4*, 209. (b) Kiessling, R. *Acta Chem. Scand.* **1949**, *3*, 603.
(3) Widera, A.; Eisenmann, B.; Schäfer, H.; Turban, K. *Z. Naturforsch. B* **1976**, *31B*, 1592.
(4) Widera, A.; Schäfer, H. *Z. Naturforsch. B* **1979**, *34B*, 1769.
(5) Klepp, K.; Parthé, E. *Acta Crystallogr., Sect. B* **1982**, *38B*, 2026.

0022-3654/88/2092-0887$01.50/0

TABLE I: Some Reported $M_3A_2E_2$ Structures of the $Ca_3Al_2Si_2$ Type

formula	A–A, Å	A–E, Å	ref
$Ca_3Al_2Si_2$	2.469	2.434	1
$Sr_3Al_2Si_2$	2.530	2.460	1
$Ba_3Al_2Si_2$	2.518	2.500	1
$Ca_3Al_2Ge_2$	2.510	2.510	3
$Sr_3Al_2Ge_2$	2.560	2.550	3
$Ba_3Al_2Ge_2$	2.660	2.550	3
$Sr_3Al_2Sn_2$	2.569	2.699	4
$Ba_3Al_2Sn_2$	2.571	2.768	4
Y_3NiSi_3	2.295	2.381	5

band calculations, with parameters specified in the Appendix.

The Electronic Structure and Stability of the $Al_2Si_2^{6-}$ Chain

The unit cell of an $Al_2Si_2^{6-}$ chain contains four atoms, two of which are aluminums, and the other two are silicons. Several ways are possible to accommodate these four atoms into the available twofold and threefold sites. Depicted in **4** are the three which we denote as configuration I, II, and III. Configuration I is the

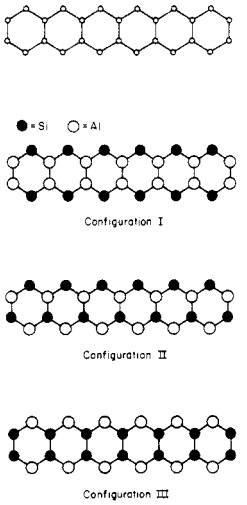

4

experimentally observed structure with all Al atoms in threefold sites and all Si atoms two-coordinate. Configuration III, on the other hand, represents the opposite choice, where Al and Si atoms in configuration I exchange their positions. Also considered is one intermediate case, configuration II, in which aluminums and silicons share the twofold and threefold sites equally.

It is not obvious why the experimentally observed structure was chosen, or what in fact is the order of thermodynamic stability of these isomeric lattices. Questions of this type, of site preferences, isomer stability or "the coloring problem"[7] arise frequently in chemistry.[8]

There are several ways to approach the isomer stability problem in this case. One way is the use of the moment method, introduced by Burdett and Lee.[10] This approach indeed leads to conclusions about the stability of this structure similar to ours based on the orbital methods.[11] Our orbital approach is first to recognize the inherent electronic asymmetry of the AB unit $AlSi^{3-}$ from the beginning and to build up the electronic structure of the $A_2B_2^{6-}$

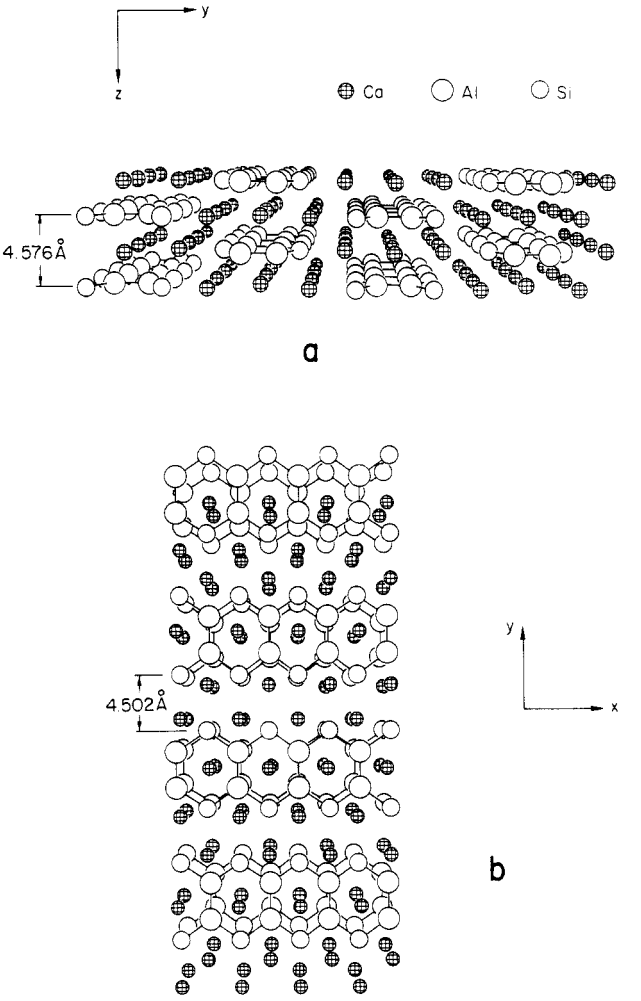

Figure 1. Two perspective views of the $Ca_3Al_2Si_2$ structure: (a) seen along x axis, (b) along z axis.

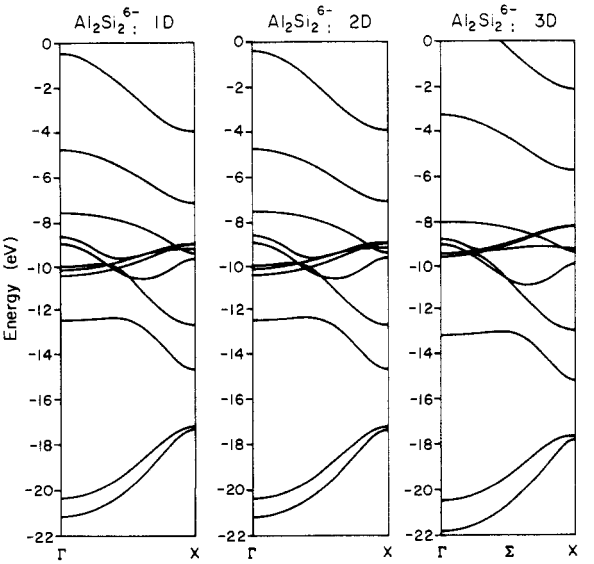

Figure 2. Calculated band structure along the chain axis for the $Al_2Si_2^{6-}$ one-dimensional, two-dimensional, and three-dimensional structures.

(6) (a) Hoffmann, R. *J. Chem. Phys.* **1963**, *39*, 1397. Hoffmann, R.; Lipscomb, W. N. *J. Chem. Phys.* **1962**, *36*, 2179, 3489; **1962**, *37*, 2872. Ammeter, J. H.; Burgi, H.-B.; Thibeault, J. C.; Hoffmann, R. *J. Am. Chem. Soc.* **1978**, *100*, 3686. (b) Whangbo, M.-H.; Hoffmann, R. *J. Am. Chem. Soc.* **1978**, 6093.

(7) Burdett, J. K.; Lee, S.; McLarnan, T. J. *J. Am. Chem. Soc.* **1985**, *107*, 3083.

(8) See, for example: (a) Ito, T.; Morimoto, N.; Sadanaga, R. *Acta Crystallogr.* **1952**, *5*, 775. Minshall, P. C.; Sheldrick, G. M. *Acta Crystallogr., Sect. B* **1978**, *34B*, 1326. Sharma, B. D.; Donohue, J. *Acta Crystallogr.* **1963**, *16*, 891. (b) Smith, G. S.; Johnson, Q.; Nordine, P. C. *Acta Crystallogr.* **1965**, *19*, 668. (c) Nolle, D.; Noth, H. *Z. Naturforsch. B* **1972**, *27B*, 1425. Noth, H.; Ullmann, R. *Chem. Ber.* **1975**, *108*, 3125. (d) Albright, T. A.; Burdett, J. K.; Whangbo, M.-H. *Orbital Interactions in Chemistry*; Wiley: New York, 1985. (e) Zheng, C.; Hoffmann, R. *J. Am. Chem. Soc.* **1986**, *108*, 3078. Burdett, J. K.; Canadell, E.; Hughbanks, T. *J. Am. Chem. Soc.* **1886**, *108*, 3971. (f) Burdett, J. K. *J. Am. Chem. Soc.* **1980**, *102*, 450.

(9) For some applications see: (a) Wijeyesekera, S. K.; Hoffmann, R. *Organometallics* **1984**, *3*, 949. (b) Kertesz, M.; Hoffmann, R. *J. Am. Chem. Soc.* **1984**, *106*, 3453. (c) Saillard, J.-Y.; Hoffmann, R. *J. Am. Chem. Soc.* **1984**, *106*, 2006.

(10) Burdett, J. K.; Lee, S. *J. Am. Chem. Soc.* **1985**, *107*, 3050.

(11) Burdett, J. K. *Struct. Bonding* **1987**, *65*, 29.

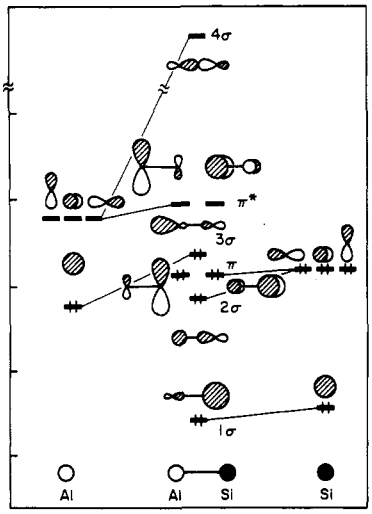

Figure 3. Schematic orbital interaction diagram for the $AlSi^{3-}$ monomer. The Al atomic orbitals are drawn at left and the Si atomic orbitals at right.

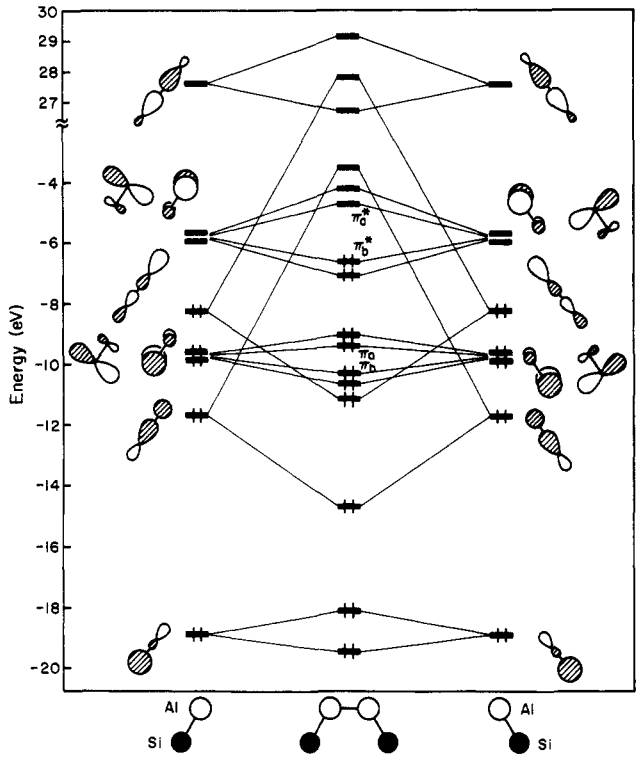

Figure 4. Schematic diagram showing the orbital interactions when two $AlSi^{3-}$ monomers are brought together to form a bond between two Al atoms.

isomers by assembling these from the AB puzzle pieces fitting together in different ways, **5**. Alternatively we can use the symmetric polyacene or A_4 or B_4 structure as a starting point and

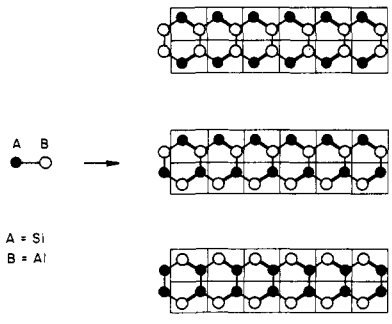

5

see to what an asymmetric electronegativity perturbation is likely to lead. This is indicated schematically in **6**.

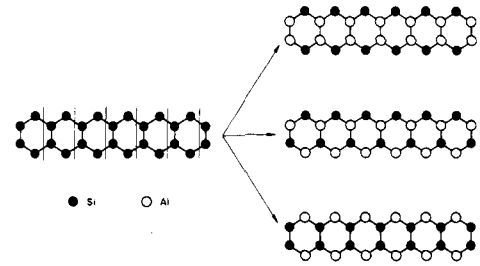

6

We begin with the first approach, from AlSi. The schematic orbital interaction diagram for the $AlSi^{3-}$ monomer is constructed in Figure 3. The more electronegative Si atom interacts with the more electropositive Al atom to form eight molecular orbitals. The lower four of these, 1σ, 2σ, and π, are concentrated on Si 3s and 3p; and the upper four, 3σ, π^*, and 4σ, are more Al-like. Notice that here the highest occupied molecular orbital is 3σ.

The construction principle we should like to follow is **7** → **8** → **9**. Step **8** is accomplished in Figure 4. The perturbation of forming the $Al_2Si_2^{6-}$ dimer is very strong, so that the level ordering of Figure 4 is quite different from that of Figure 3.

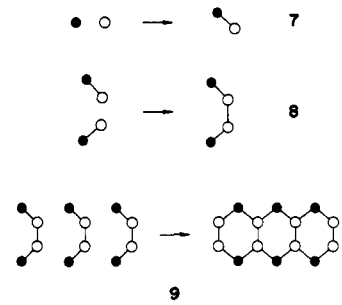

Now the HOMO is π_b^* and LUMO is π_a^*. The subscripts b and a stand for "bonding" and "antibonding" between the two $AlSi^{3-}$ units. It is apparent from Figure 4 that all the degeneracies are removed. The splitting of the π orbitals of the two monomers is small but that of the π^* orbitals is big. This is understandable from the electronegativity difference of an Al and a Si atom and its effect on the localization of the π-type orbitals. The π-orbital is localized on the more electronegative atom, Si, but the a–b splitting is through Al–Al interactions. Note also that the highest occupied orbital is stabilized.

From now on we will concentrate on the π and π^* orbitals, for it is from these that the differences in isomer stabilities derive. Next is the polymer formation indicated in **10**. Each unit cell

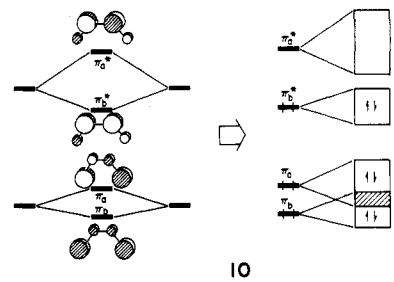

10

level in the $Al_2Si_2^{6-}$ monomer should broaden into a band. The process for the four π levels is shown in **10**. The energy difference between π_b and π_a on the left of **10** is so small that one expects that an overlap of the two corresponding bands should occur in the polymer at the right. The π_b^* and π_a^* levels, however, are so far apart that the bands of these levels in the polymer are probably separated by an energy gap.

Up to now, our analysis has focused on configuration I. The same line of reasoning can be applied to configuration II and III. In Figure 5, comparisons are made of the π-type orbitals for all

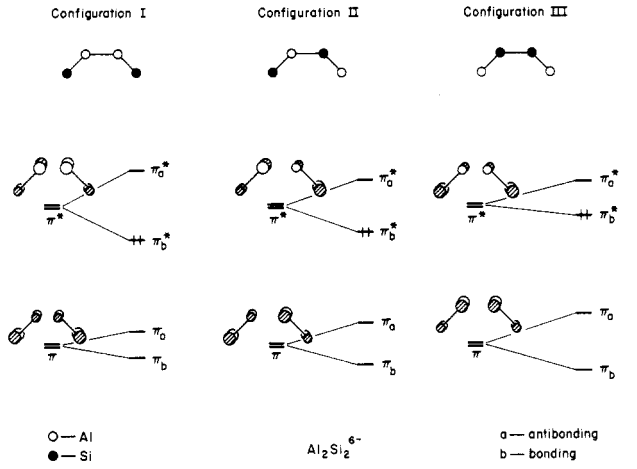

Figure 5. π-type interactions in configuration I, II, and III.

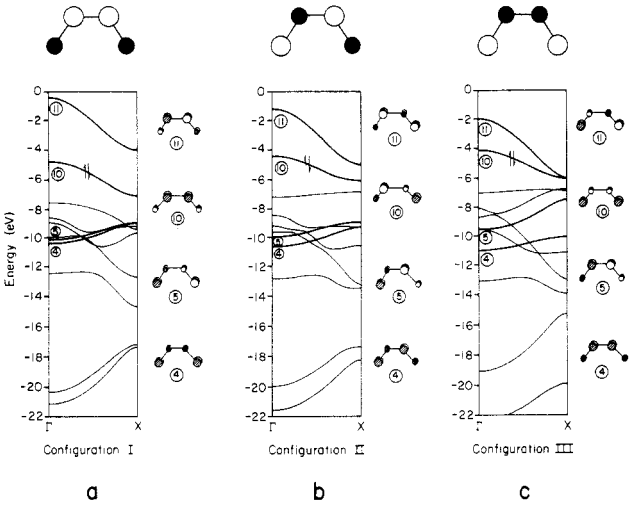

Figure 6. Calculated band structure for $Al_2Si_2^{6-}$ chain: (a) configuration I, (b) configuration II, and (c) configuration III. The π-bands are emphasized by heavy lines. The corresponding orbitals at Γ are drawn in the figure.

three configurations. The trend is clear: the energy difference between the π_b and π_a levels, that is, the bonding and antibonding combinations of the $AlSi^{3-}$ π-orbitals, should get bigger as one proceeds from I to III. The opposite trend is expected for the bonding and antibonding combinations of the $AlSi^{3-}$ π^* orbitals, i.e., the π_b^* and π_a^* levels. The direct consequence of this is that the highest occupied orbital π_b^* is lower in energy for configuration I than for configuration III, or π_b^* (I) < π_b^*(II) < π_b^*(III).

What about the total energy of these isomers? Often the highest occupied orbital determines the stability of a molecule; Similarly in an extended system the highest filled band is likely to be important in setting the Fermi energy and relative stability. In the case at hand both π-levels are filled, and so the fact that there is more or less splitting among them is not likely to affect the total energy but of the two π^*-bands, only π_b^* is filled, and the isomer stability order should follow the stabilization of π_b^*, i.e., I more stable than II more stable than III. Let us see how this simple explanation holds up when one looks at actual band calculations.

Parts a, b, and c of Figure 6 are the calculated band structures for configuration I, II, and III, respectively. The π-type orbitals are in dark and are drawn at the Γ point for all three. These orbitals are in good agreement with those shown in **10** and Figure 5. Notice the small band gap between the 10th and the 11th band in Figure 6a and the overlap between these bands in Figure 6, b and c. The trends we discussed above are apparent. The bandwidth of the π-block (π_b and π_a) is increased dramatically from configuration I to III. If other, σ-type, bands are ignored, a gap between π_b and π_a should occur in the configuration III. The 10th band, the valence band or the "HOMO", in the sense

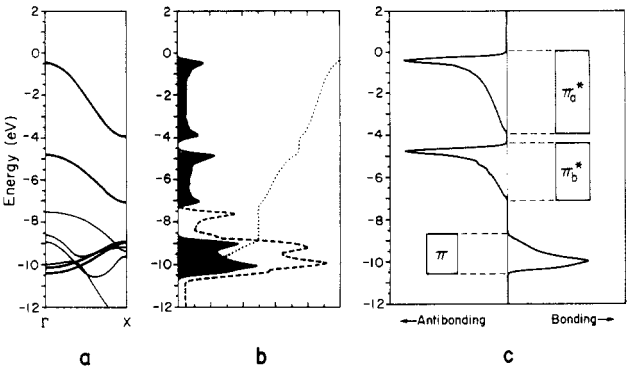

Figure 7. Band structure and DOS and COOP curves for configuration I of the $Al_2Si_2^{6-}$ chain: (a) band structure; (b) DOS, the black area is in the π contribution; the dashed line, total DOS; and the dotted line, the integration of the π-states; (c) COOP curve of the π-orbital contributions to Al–Si bond.

TABLE II: Average Total Energy (eV) per Unit Cell for All Three Configurations

structure	configuration I	II	III
$Al_2Si_2^{6-}$	[0]	2.9	6.4
$Al_2Ge_2^{6-}$	[0]	3.2	5.4
$Al_2Sn_2^{6-}$	[0]	1.8	3.9

that it is entirely or mostly filled, has an energy of −4.8, −4.4, and −4.1 eV at its top Γ for configuration I, II, and III respectively.

Another way to probe the bonding in extended structures is to construct crystal orbital overlap population (COOP)[9] curves. These bonding indicators are really overlap population weighted densities of states. Figure 7 shows side by side the band structure, DOS, and the π-orbitals contribution to the Al–Si COOP for configuration I. Note the clear Al–Si bonding in the lower band (π_a and π_b overlapping), and the Al–Si antibonding in the upper band.

The total energy per unit cell that we calculate (Table II) follows the expectations: configuration I is more stable than II, which in turn should be more stable than III. Similarities, shown in Table II as well, obtain for $Al_2Ge_2^{6-}$ and $Al_2Sn_2^{6-}$.

The extra stability of configuration I over III can be understood also from another point of view. Drawn in **11** are schematic band diagrams for the two isomeric polymers. The Fermi level is

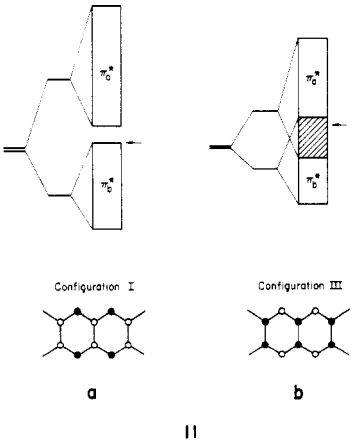

11

indicated by an arrow. The band corresponding to the antibonding combinations of the $AlSi^{3-}$ π^*-orbitals, π_a^*, is filled substantially in **11b** but is empty in **11a**. The filling of an antibonding orbital in a molecule, or of an "antibonding" band in a solid, should result in an increase in energy and, consequently, a destabilization of the structure.

The calculations indicate that the observed structure should be a semiconductor. The as yet unsynthesized isomers might be metallic, or they might deform, in ways which could be easily examined, via a Peierls distortion.

Site Preference of Si and Al in the $Al_2Si_2^{6-}$ Chain

Si clearly prefers the twofold site and Al the threefold one in this structure type. Can we fit this experimental preference, theoretically confirmed above, into the general theories that one has for substituent site preferences?

One idea which has found great utility is that if a parent structure has nonequivalent substitution sites, which will naturally differ in electron density, then the more electronegative substituent will preferentially enter the sites with greater electron density.[7,12] This has been called the rule of topological charge stabilization by Gimarc[13] who has given many examples. Burdett has extended this idea to solid-state problems, for example, the B_2C_2 net in the ScB_2C_2 structure. His calculation on the C_4 net of the same geometry indicates that the C atoms do occupy the sites of higher electron density.[14]

A calculation on a Si_4^{4-} chain in the $Al_2Si_2^{6-}$ structure gives the total electron distribution of **12**. The π-electron density (also

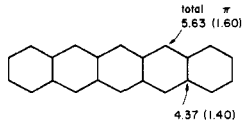

12

indicated) follows the same order, but is more attenuated. Thus it is clear that the less electronegative Al atoms should enter the threefold sites, and they do.

Another way to reason about site preferences in the solid state is in terms of the dispersivity of nonequivalent lattice sites.[15] The argument goes as follows: First dispersivity is defined. Suppose the crystal lattice is composed of nonequivalent sublattices. The bandwidth of the relevant orbitals of each individual sublattice is examined. This width depends on (a) the number of nearest neighbors in the sublattice, and (b) the distances to those neighbors. The more neighbors and the shorter the separations, the greater the width or dispersion of the band generated by that sublattice. We would then say that lattice site (i) or sublattice (i) is more dispersive than lattice site (ii), etc.

Suppose different elements have a choice of entering different lattice sites. The Fermi level will be set by the ordering in energy of the elements, by their electronegativity. Probably only the band or bands at or near the Fermi level will matter in setting geometry preferences: this is a cardinal assumption of frontier orbital theory. The site dispersivity line of reasoning is that if the Fermi level is at the middle of or below the middle of the valence band and that the element which is mainly responsible for that band should enter the most dispersive site (most number of near neighbors, shortest contacts within sublattice). But if the band is more than half-filled the element generating the band should enter the least dispersive site.

This approach sounds more cumbersome than it is. In the $Al_2Si_2^{6-}$ case at hand, the electronegativity order is Si > Al, so the Al-based bands will be at higher energy, as indicated schematically in **13**. The Fermi level corresponds to 10 electrons

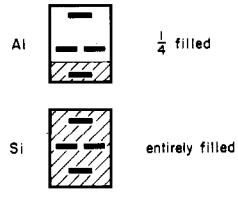

13

per AlSi, or to total filling of the "Si" band, $^1/_4$ filling of the "Al" band. The threefold site is obviously more dispersive than the twofold site. The AlSi building block of **13** will then develop into bands as indicated in **14**. Notice the difference in Fermi energy for the two configurations. Configuration I is favored.

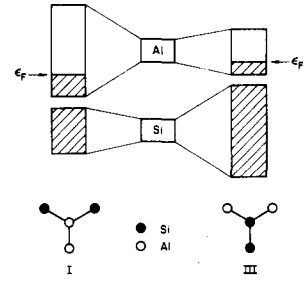

14

It may seem at first sight as if the argument based on the rule of topological charge stabilization is simpler than the one based on dispersivity. Not really. The dispersivity argument explicitly considers the electron count, and its crucial importance. The simple statement of the topological charge stabilization rule seems to ignore the extent of electron filling. But of course it must consider it—the electron distribution in the parent structure is a sensitive function of the total electron count. Gimarc gives some neat examples of this for heteroatom-substituted pentalenes and pentalene dianions.[13]

The $Al_2Si_2^{6-}$ Chain and the Related Organic Analogue, Polyacene

As we mentioned before, the $Al_2Si_2^{6-}$ chain is closely related to the organic polymer, polyacene. In fact, one may easily derive the $(Al_2Si_2^{6-})_\infty$ structure from polyacene. The polyacene unit cell consists of a C_4H_2 unit, which is isoelectronic to C_2N_2 or C_4^{2-}. $Al_2Si_2^{6-}$, on the other hand, is just like Si_4^{4-}, or C_4^{4-}. It has two more π-electrons per unit cell over the polyacene count. Alternatively, replacing the two CH unit in polyacene by two Si^- and the C_2 by Al_2^{2-}, and adding two π-electrons to the polyacene, gives rise to the $Al_2Si_2^{6-}$ chain structure. The electronic structure of polyacene is by now very well-known.[16] A variety of derivations of the π bands of this system are available. In a simple Hückel treatment[14] the π-orbitals of butadiene are used as a starting point, "polymerization" of butadiene, **15**, produces the polyacene chain. We have already followed this construction principle.

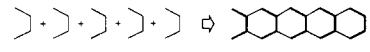

15

A recent paper by Lowe and co-workers[17] provides us with another way of tackling the same problem. In his instructive paper polyacene is constructed by making a bond at every other carbon between two *trans*-polyacetylene chains, **16**. Similar qualitative

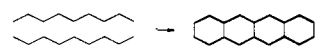

16

constructions are available from Burdett and Whangbo.[14,16c] We would like to make use of these simple ideas and arguments to produce a qualitative π-band structure of our $Al_2Si_2^{6-}$ chain without employing any calculations and compare to it, step by step, with same process for polyacene. This way we hope to gain a better understanding of the similarities and dissimilarities of the two systems.

(12) For example, see: Chen, M. M. L.; Hoffmann, R. *J. Am. Chem. Soc.* **1976**, *98*, 1647. Hoffmann, R.; Howell, J. M.; Muetterties, E. L. *J. Am. Chem. Soc.* **1972**, *94*, 3047.

(13) Gimarc, B. M. *J. Am. Chem. Soc.* **1983**, *105*, 1979.

(14) Burdett, J. K. *Prog. Solid State Chem.* **1984**, *15*, 173.

(15) (a) Hoffmann, R.; Zheng, C. *J. Phys. Chem.* **1985**, *89*, 4175. (b) Zheng, C.; Hoffmann, R.; Nesper, R.; Schnering, H.-G. *J. Am. Chem. Soc.* **1986**, *108*, 1876.

(16) See, for example: (a) Whangbo, M.-H.; Hoffmann, R.; Woodward, R. B. *Proc. R. Soc. London* **1979**, *A366*, 23. (b) Kertesz, M.; Hoffmann, R. *Solid State Commun.* **1983**, *47*, 97. (c) Whangbo, M.-H. In *Crystal Chemistry and Properties of Materials with Quasi-One-Dimensional Structures*; Rouxel, J., Ed.; Reidel: Dordrecht, Holland, 1986, pp 27–85. (d) Reference 12.

(17) Lowe, J. P.; Kafafi, S. A.; LaFemina, J. P. *J. Phys. Chem.* **1986**, *90*, 6602.

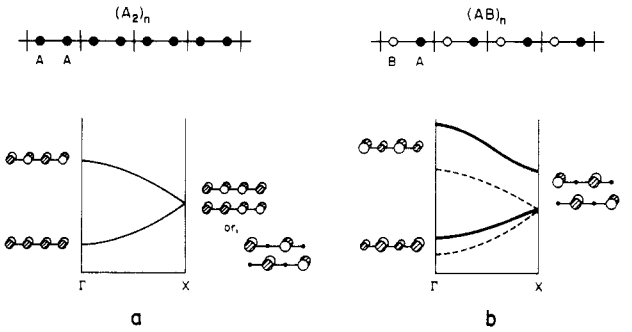

Figure 8. Construction of the π-bands for (a) an A_2 chain and (b) an AB chain.

Let us begin with a diatomic molecule as the basic construction material. It is well-known that when two atoms of same type, e.g., A, interact to form a homonuclear molecule A_2, the molecular orbitals so formed have equal contributions from the two atoms. However, when the two atoms A and B are different, it would be atom A that is weighed more in bonding molecular orbitals if it is more electronegative than B. The situation is reversed for the antibonding MO's. These are sketched in **17** for a π-type interaction. Next, we take the A_2 and AB as a repeating unit

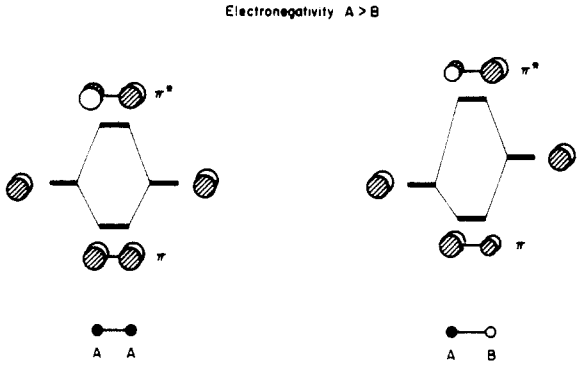

17

and form infinite chains $(A_2)_\infty$ and $(AB)_\infty$ by linking up these diatomic units. The corresponding π-bands are constructed in Figure 8.

For the homonuclear A_2 polymer the band structure is obvious—a simple band "folded-back" as a result of doubling the basic electronic unit.[8d,14,16c] The degeneracy at $k = \pi/a$, X, is a consequence of an assumption that the chain is equally spaced, i.e., the inter-unit-cell A–A distance is the same as the intra-unit-cell one.

The same linear combinations are stipulated by the Bloch functions for the AB polymer. We can estimate the perturbation in energy from the A_2 case by examining in detail the behavior at specific k points. The perturbation is that B is less electronegative than A. This lifts all the orbitals up in energy, throughout the zone, but with important special consequences at the zone edge. The linear combinations there can be written in two ways, and are drawn in **18** for the case of A_2 polymer. The $\Psi_\pm$ choice makes

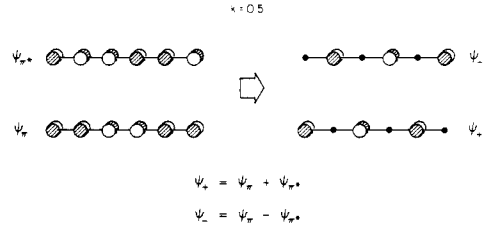

18

it clear why substituting a B atom breaks the degeneracy of the homonuclear case, lifting one orbital up at X.

Now that we have the bands for both A_2 and AB chains we go on to build up the $(A_4)_\infty$ and $(A_2B_2)_\infty$ structures which are

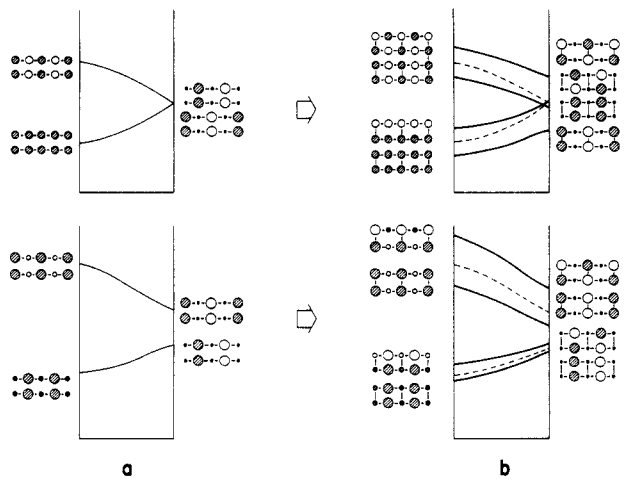

Figure 9. Construction of the π-bands for (a) an $(A_4)_\infty$ system from two parallel A_2 chains, (b) an A_2B_2 chain from two parallel AB chains. Crystal orbitals are sketched at two special k points, i.e., $k = 0$ and $k = 0.5$.

relevant to the polyacene and $Al_2Si_2^{6-}$ chain. The process is described in **19**. To obtain a $(A_4)_\infty$ type structure, one makes

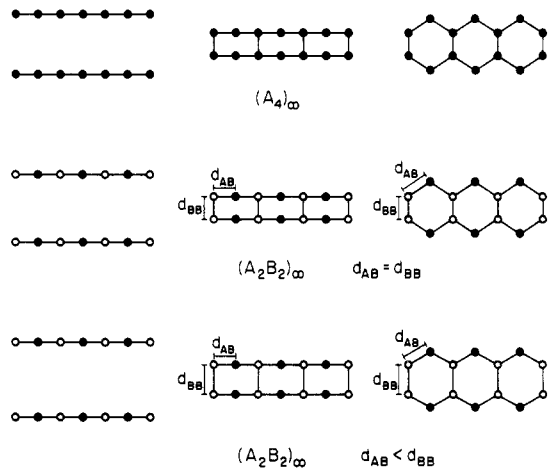

19

a bond between every other pair of atoms from the two identical A_2 chains. The $(A_2B_2)_\infty$ structure can be constructed in the same way, but with connections between the B–B pairs only. Equal A–B and B–B distances are at first assumed; The real structure can be reached by the small perturbation of making these distances unequal. Figure 9 follows the process described in **19**.

The two $(A_2)_\infty$ bands split into bonding and antibonding combinations as a consequence of interactions between the chains. The splitting is bigger for the band of higher energy than for the band of lower energy. The degeneracy at the zone edge is removed when the overlap between the two non-nearest-neighbor A atoms in the unit cell is taken into account.[14] But the two levels should stay close in energy, since the interaction is weak. A crossing occurs near X; the two bands involved are of different symmetry with respect to the reflection plane perpendicular to the molecular plane and containing the chain axis.

The splitting pattern for the AB chain can be derived in a similar fashion. Here some differences emerge. One thing is that no crossing occurs nor any avoided crossings. Another thing one observes is that the splitting of the lower band is much smaller than the upper band. This is understandable from the electronegativity difference between atom A and B. Upon formation of an A_2B_2 double chain, the connections are to be made between B atoms from the two parallel AB chains. These atoms, due to their electropositivity, contribute much less to the lower band than do the A atoms. Therefore, the $(A_2B_2)_\infty$ crystal orbitals should have a small overlap between every B–B pair for the two lower

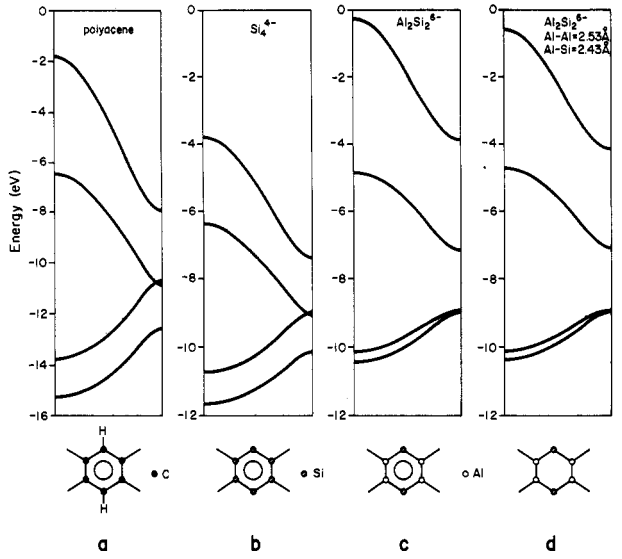

Figure 10. Calculated π-bands for (a) polyacene, (b) Si_4^{4-} chain, (c) $Al_2Si_2^{6-}$ chain with equal A–B and B–B distances, and (d) $Al_2Si_2^{6-}$ chain with $d_{BB} > d_{AB}$.

bands but a large overlap for the two upper bands. As a result, the splitting is substantial between the upper two but is small for the lower two.

The orbitals drawn beside the bands of Figure 9 may help with the argument. These are the crystal orbitals for the A_2B_2 chain at two special k points, i.e., $k = 0$ and $k = 0.5$. The two lower bands at Γ have small lobes on B and have no contributions from these atoms at X. The situation is reversed for the two upper bands at both Γ and X. Also notice the greater extent of the band splitting at Γ than at X. This is clear from the way in which orbitals are drawn. For instance, let us take a close look at the two lower energy orbitals, resketched in **20**. First we concentrate

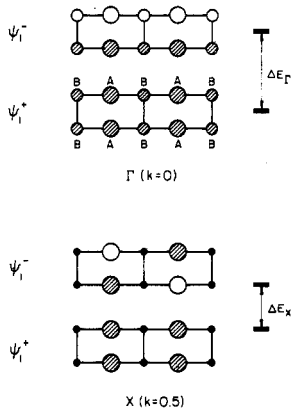

20

on those at the Γ point. The energy lowering of Ψ_1^+, which is small according to the discussions given above, mainly comes from the B–B interaction, since a bond is formed between the two atoms. The A–A interaction, although in-phase, and with large lobes on the atoms, is weak and indirect, for no bond is made between the two. Thus, the effect of such interaction on the energy is only of second order. The same reasoning may be used for Ψ_1^-. Now we turn to the corresponding orbitals at X. Here the only interaction present is between the nonbonded A atoms, a second order, indirect type. So the energy difference between Ψ_1^- and Ψ_1^+ should be very small.

TABLE III: Atomic Parameters Used in the Calculations

atom	orbital	H_{ii}, eV	ζ
Si	3s	−17.30	1.38
	3p	−9.20	1.38
Al	3s	−12.30	1.17
	3p	−6.50	1.17
H	1s	−13.60	1.30

Finally, we show in Figure 10 the calculated π-bands for polyacene and for Si_4^{4-} chain; Also shown in the figure are the $(Al_2Si_2^{6-})_\infty$ π-bands with $d_{BB} = d_{AB}$ and $d_{BB} > d_{AB}$. The latter corresponds to the experimental geometry. That the small perturbation in the B–B bond length gives rise to a smaller splitting of both lower and upper band of the $(AB)_\infty$ can be seen from the corresponding bands in the figure.

We have now generated the orbitals of polyacene or an A_4 system, and its substituted AB derivative; The correspondence to the previously generated $Al_2Si_2^{6-}$ orbitals is quite exact. Perhaps it is worthwhile to repeat here that polyacene and $Al_2Si_2^{6-}$ have different electron counts. In the hydrocarbon only the two lower π-bands are filled; in $Al_2Si_2^{6-}$ the third, π^*-band is also occupied.

The main purpose of the argument of this section is to provide us with the confidence in a qualitative, perturbation theory based construction of the orbitals of this simple polymeric system. The methodology, outlined in detail here, can be followed for other, more complex, extended structures.

Acknowledgment. We are grateful to the National Science Foundation for its generous support of this work through grant CHE 8406119. We thank Jane Jorgensen and Elisabeth Fields for their expert drawings.

Appendix

All the calculations are of the extended-Hückel-type tight-binding approach. The atomic parameters for Si, Al, and H atoms are tabulated in Table III. The experimentally determined geometry is used for the $Al_2Si_2^{6-}$ chain and the data for polyacene are taken from Tyutyulkov et al.[18]

Registry No. $Ca_3Al_2Si_2$, 66057-98-5.

(18) Tyutyulkov, N. N.; Polansky, O. E.; Fabian, J. *Z. Naturforsch. A* **1975**, *30A*, 1308.

(19) In this paper the periodic group notation in parentheses is in accord with recent actions by IUPAC and ACS nomenclature committees. A and B notation is eliminated because of wide confusion. Groups IA and IIA become groups 1 and 2. The d-transition elements comprise groups 3 through 12, and the p-block elements comprise groups 13 through 18. (Note that the former Roman number designation is preserved in the last digit of the new numbering: e.g., III → 3 and 13.)